© EARSeL and Warsaw University, Warsaw 2005. *Proceedings of 4th EARSeL Workshop on Imaging Spectroscopy. New quality in environmental studies*. Zagajewski B., Sobczak M., Wrzesień M., (eds)

SUBPIXEL INFORMATION ON DIRECTIVITY OF SOIL SURFACE SHAPE

Jerzy Cierniewski[1], Tomasz Gdala[2]

1. Adam Mickiewicz University, Department of Soil Science and Remote Sensing of Soils, Poznan, Poland; ciernje@amu.edu.pl
2. Adam Mickiewicz University, Mathematics and Computer Science Faculty, Poznan, Poland; tgdala@amu.edu.pl

ABSTRACT

While modelling the hemispherical-directional reflectance of soil surfaces with different shape, it was found that their hemispherical-directional reflectance function (HDRDF*)* not only includes general information about their shape, i.e. that it is more or less rough, but this function also contains further details, such as its directivity (i). The directivity of soil surface geometry can be obtained by analysing the symmetry of the HDRDF with respect to the solar principal plane. The HDRDF of surfaces, with an indirect, random spread of their height irregularities, is almost symmetrical. However, the HDRDF of surfaces with directional microrelief-like furrows is asymmetrical: the greater the asymmetry, the stronger the directional character of the surfaces. Thus, analysing brightness variation of a soil surface image viewed by a sensor at specific directions in definite illumination conditions, it is possible to infer the surface shape directivity even at a scale which makes it impossible to perceive the directivity features for the reason that they are too detailed in relation to the image pixel size. The paper, analysing variation of the HDRDF function of surfaces with bigger and bigger deepening furrowed microrelief focuses on the problem in which illumination and viewing conditions inferring the shape directivity of these surfaces become available using remote sensing methods.

INTRODUCTION

Wave energy reflected from bare soil surfaces in the optical range is distributed non-equally in all directions. Their reflectance varies due to the directions of its illumination and observation. Description of the soil surface reflectance by the bidirectional reflectance distribution function (BRDF), as the ratio of radiance reflected by the surface to the incident irradiance from only one source of illumination, shows that most soils with dominant diffuse features display a clear backscattering character with a reflectance peak towards the light source position and decreasing reflectance in the direction away from the peak (ii). The peak of backscattering radiation becomes less pronounced at a low zenith angle of the light source. Irregularities of these surfaces make it impossible to completely illuminate them. Part of the light coming from this one point source to a fragment of the soil surface can be blocked by the presence of its adjoining fragments. These fragments, being usually larger than wavelengths in the optical domain and opaque, cast shadows on the surface. Wave energy leaving the shaded areas, at the most being illuminated by the energy reflected earlier from other non-shaded fragments, is many orders-of-magnitude smaller than the energy reflected from its fragments directly illuminated by this one light source. Variation of the shadow is the main reason for their non-Lambertian behaviour. The surfaces seem to be the brightest from the direction which gives the lowest proportion of the shaded fragments. Desert soil materials with specular features, like gypsum sand and beach quartz sand, display a high reflectance with a strong forwardscattering character, which varies with the angle of the incident radiation, reaching its maximum at the highest zenith angles (iii).

If these surfaces are illuminated by more than a single light source, as in natural field conditions by the direct solar and the diffuse sky, their non-equal reflectance distribution is less manifested. The lower the non-Lambertian effects, the higher the proportion of this diffuse component, because magnitude of the energy reflected from the sunlit fragments becomes similar to the amount of energy leaving the shaded parts. The proportion of the diffuse light in the global skylight decreases

with the wavelength and depends on atmosphere state, cloudiness and contents of aerosols and their quality. The distribution of the sky radiation environment incoming to Earth surfaces, like the distribution of the radiation reflected from them, is unequal. Ground measurements, carried out in a desert region of the state of New Mexico, show that in clear sky condition for clean atmosphere the sky is very bright near the sun in the so-called aureole. The sky is relatively bright along the horizon, while it is the darkest in the quadrant opposite to the sun (iv). The variation of the sky radiance intensity becomes lower when the sun elevation rises. Kondratyev (v) has mentioned that the variation could be practically negligible for sun elevation angles higher than 60°. When the sky is completely overcast, the radiance distribution is almost constant with its weak monotonic drop from the zenith to the horizon.

Abdou et al. (vi) and Strub et al. (vii) suggest that practical data about the directional reflectance behaviour of different objects, that have been collected so far, require the use of the hemispherical-directional reflectance approach (viii), rather than the bidirectional reflectance one, as the incident irradiance under conditions of outdoor illumination consists of a mixture of direct solar and non-isotropic diffuse components.

While modelling the hemispherical-directional reflectance of soil surfaces with their different height irregularities caused by texture, aggregates and microrelief configuration, formed by farming tools, it was found that their hemispherical-directional reflectance function (HDRDF*)* not only includes general information about their shape, i.e. that it is more or less rough, but the function also contains further details, such as its directivity (i). The directivity of soil surface geometry can be obtained by analysing the symmetry of the HDRDF with respect to the solar principal plane. The HDRDF of surfaces, with an indirect, random spread of their height irregularities, is almost symmetrical. However, the HDRDF of surfaces with directional microrelief-like furrows is asymmetrical: the greater the asymmetry, the stronger the directional character of the surfaces. This relationship between the directivity of soil surface shape and the directivity of the surface hemispherical-directional reflectance distribution function was confirmed on an example of soil, *Calcic Xerosols* developed from sandy loam. The surface, situated in a field of an experimental agricultural farm near Beer Sheva in Israel (31.33°N, 34.67°E), was prepared by a cultivator which shaped furrows 10 cm deep and the distance between their successive tops of 60 cm.

The present paper focuses on the problem for which illumination and viewing conditions inferring the shape directivity of soil surfaces is available at the scale which make impossible to perceive the directivity features for the reason that they are too detailed in relation to the image pixel size. The issue is considered in the context of the directivity clarity, using the virtual surface simulating the furrowed surface, mentioned above, and others, with shallower and dipper furrows.

METHODS

These virtual surfaces are geometrical creations similar to beads merging into each other. They are characterized by three parameters a, b and c. The a and b describe its height variation along the x-axis and the y-axis, by the amplitude of the sinus function. The c expresses the disturbance in the height position in relation to the ones determined by only the a and b parameters. The virtual surface, as an opaque object, is illuminated by a hemispherical light source created by a number of point sources of given light intensities, spread equally on the hemisphere. It is assumed that for outdoor conditions the ratio of the direct solar irradiance to the global irradiance for clear sky conditions changes with the sun's position s, described by the solar zenith θ_S and azimuth ϕ_S angles, and the optical thickness of the atmosphere τ attributed to the wavelength λ. Distribution of the hemispherical light energy is described by a formula, also taking into account: the minimum amount of the energy, the amplification of the energy near the horizon, the concentration of the solar aureole and the energy at the darkest part of the hemisphere light in the quadrant opposite the sun. All these quantities are expressed by the constants, similarly as in the equation of Grant *et al.* (ix). The light energy is scattered from the surface, in accordance with the quasi-Lambertian function, being a combination of the Lambertian scattering and the quasi-specular one. The distribution of the surface hemispherical-directional reflectance $HDR(s,\tau,v)$ as viewed from all possible direc-

tions v, defined by the zenith θ_V and azimuth ϕ_V angles, can be generated for all possible illumination conditions expressed by the angles θ_S, ϕ_S and the atmosphere optical thickness τ, attributed to the given wavelength λ. It is known that variation of a soil surface reflectance is the highest between its backscatter and forwardscatter reflectance directions. Combining the concept of the backward and forward scattering with any direction ϕ we can define the HDR distribution of a soil surface as the sum of the two parts:

$$HDR_b = HDR(s,\tau,v) \text{ for } \cos\phi_V \cos\phi + \sin\phi_v \sin\phi \geq 0$$

and respectively

$$HDR_f = HDR(s,\tau,v) \text{ for } \cos\phi_V \cos\phi + \sin\phi_v \sin\phi < 0,$$

separated from each other along the line perpendicular to the ϕ direction (Fig. 1). The soil reflectance variation with respect to this line describes the absolute value of the difference between the average values of the HDR_b and the HDR_f, described by the symbol Δ_ϕ. We are looking for that ϕ angle, denoted here as the $\bar{\phi}$, for which the Δ_ϕ reaches its maximal value.

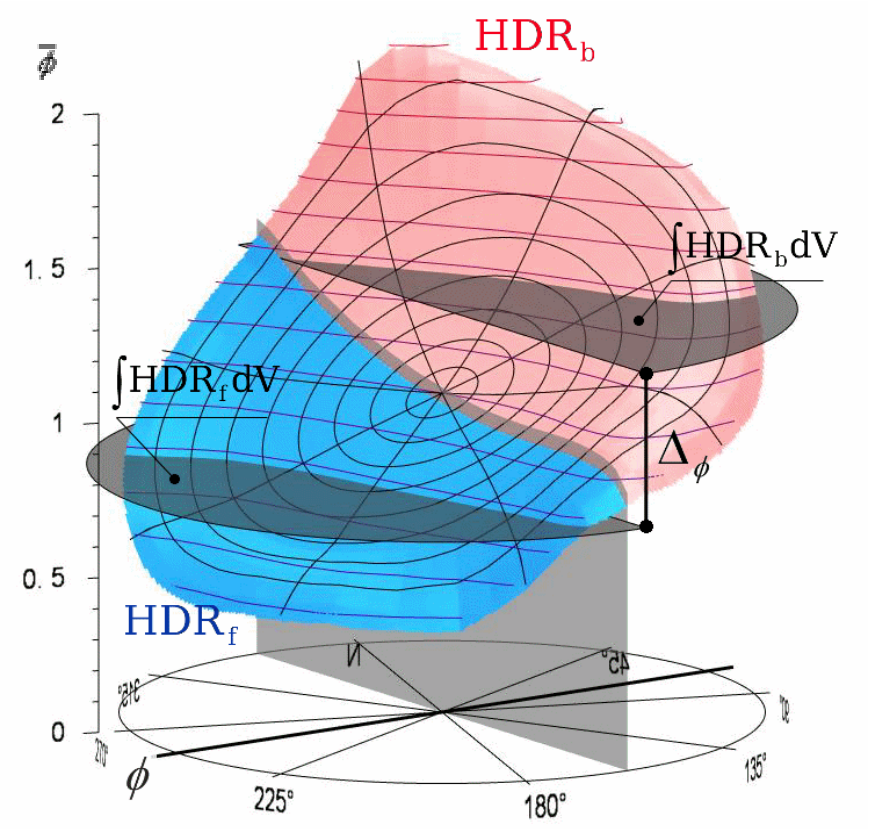

Figure 1. Two parts of the normalised to the nadir viewing hemispherical-directional reflectance HDR distribution of a soil surface, separated by the line perpendicular to a ϕ direction, the HDR_b and the HDR_f, with their average values calculated as the $\int HDR_b dV$ and the $\int HDR_f dV$, enabling us to compute the absolute value of the difference between them.

Approximating the HDR_b and HDR_f of soil surface at given illumination conditions by a specified number m of their random samples, uniformly distributed on the hemisphere, we can simulate the real way of the reflectance data collecting. The higher the m, the higher the precision of this approximation, expressed by the concentration around the black line, marked in Fig. 2. To increase the reliability of the relationship, presented in the figure, the sampling was repeated 150 times for each sample number m. The number m=25, indicated by the red line, was chosen for our investigation.

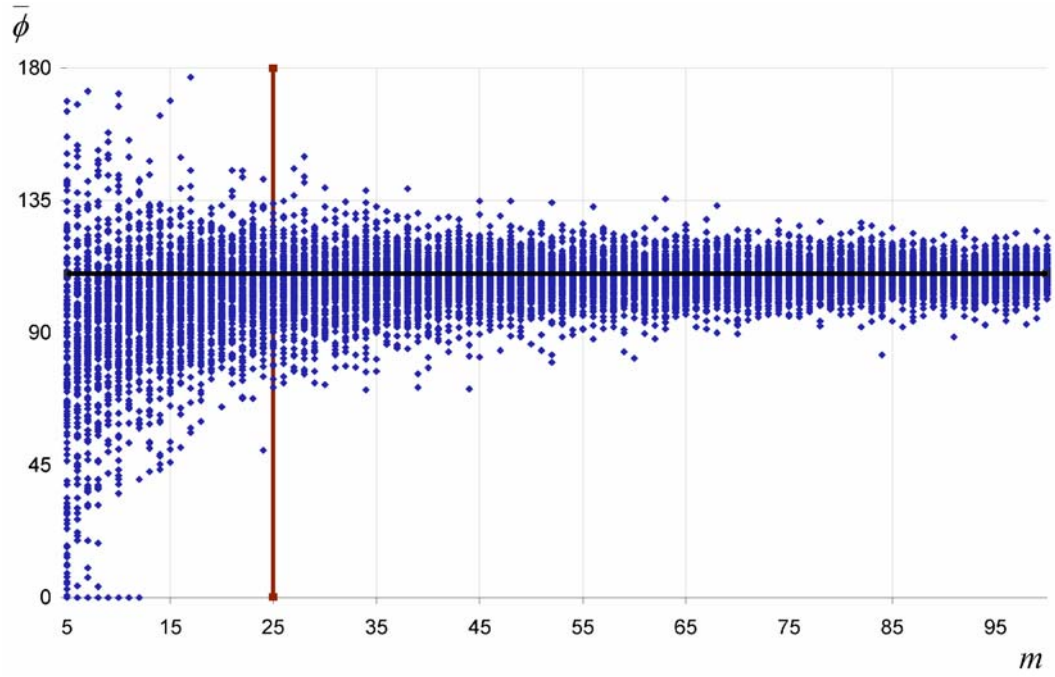

Figure 2. Relationship between the sample number m and the quality of the $\bar{\phi}$ direction approximation, considered for the soil surface example, described by the geometrical parameters: a=0.5, b=0.25, c=0.5, with its furrows illuminated at the solar zenith angle θ_S=60°and the horizontal angle $\phi_{S\text{-}C}$=45° between the direction of the furrows and the sun position in clear sky conditions characterised by the τ=0.2 attributed to the wavelength of 850nm.

RESULTS

Five virtual surfaces, one without furrows and four with furrows of their various clarity, were used to reach the goal of this paper (Fig. 3). The furrow clarity increase is expressed here by the growing values of the parameter a. The surface with relatively shallow furrows of low clarity is characterised by the a=0.25, while the surface of the deepest furrows of highest clarity is described by the a=1. One of the virtual surfaces is presented there with its real equivalent, *Calcic Xerosol*, developed from sandy loam with 0.6% of organic matter content and 16% of $CaCO_3$ content in the surface horizon. This soil, located near Beer-Sheva (31.33°N, 34.67°E) in Israel, was prepared by a cultivator which shaped 10 cm deep furrows and the distance between their successive tops of 60 cm.

In the first step of the investigation, for all the studied surfaces their hemispherical-directional reflectance HDR distributions, as viewed for all possible directions v, were generated by the model mentioned above. These distributions were predicted for the wavelength of 850 nm in clear sky conditions, described by the optical thickness of the atmosphere τ equal to 0.2, for the solar zenith angle θ_S varying from 10° to 80° at the increments of 5° and the horizontal angle $\phi_{S\text{-}C}$, describing illumination of their furrows as a distance angle between the direction of the furrows and the sun position, changing from 0° to 180° also at the increments position, changing from 0° to 180° also at the increments of 5°. These 2775 HDR distributions, were tested using the approximation method, mentioned above, to obtain their $\bar{\phi}$. Each test was repeated 150 times.

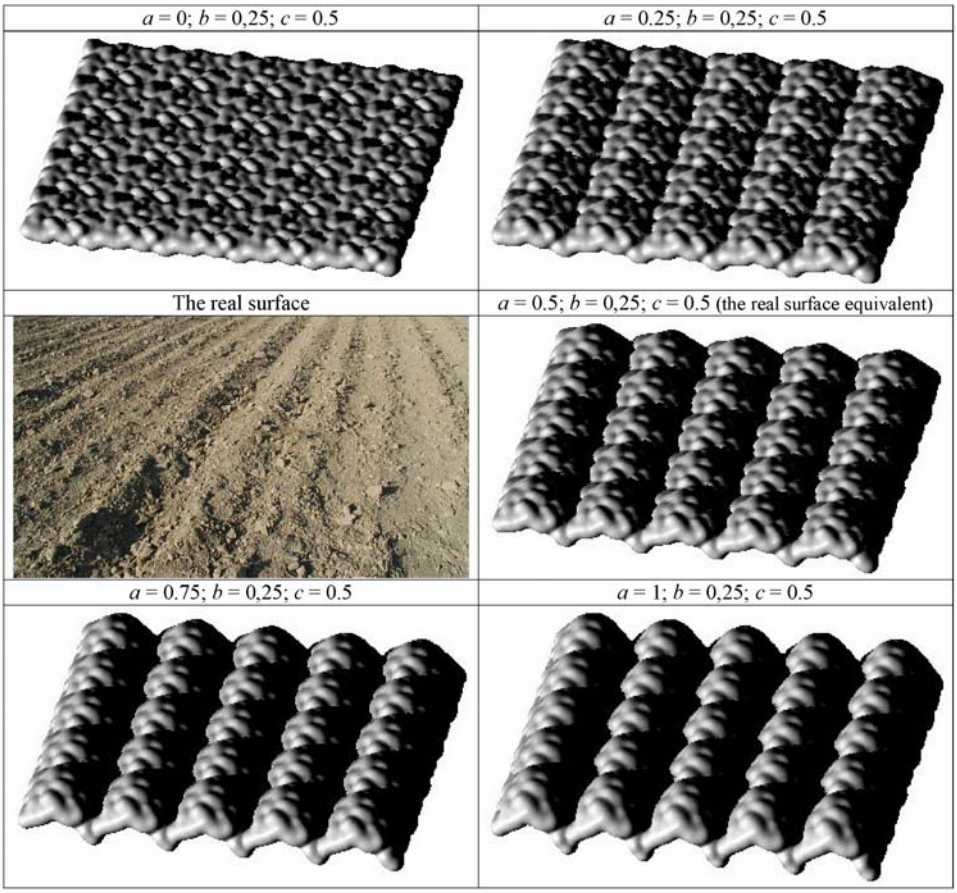

Figure 3. Virtual surfaces with varying clarity of their furrows analysed in this paper on the real equivalent background for one of them. The symbols a, b and c are the geometrical parameters of the virtual surfaces.

In the second step, the relation between the $\bar{\phi}$ and the $\phi_{S\text{-}C}$ was examined in the sets described by the surface shape and the θ_S. The character of the relation in the analysed sets clearly depends on the surface shape, as well as the solar zenith angle θ_S. Figure 4 shows this relation for the five analysed surfaces illuminated at the six specified angles θ_S: 80°, 60°, 40°, 30°, 20° and 10°. It is evident that for the surfaces with a low clarity of the furrows, described by the a~0, illuminated at sufficiently high θ_S, the relations are quasi linear. For θ_S angles lower than 30° this relation becomes inaccurate and it is more visible for surfaces with a lower clarity of the furrows than for a higher one. It was found that for the surfaces with sufficiently deep furrows, i.e. with the a>0.25, the relation between $\bar{\phi}$ and $\phi_{S\text{-}C}$ is still highly concentrated, but shaped more like the letter “S”.

We assume that the difference between $\bar{\phi}$ and $\phi_{S\text{-}C}$ expresses the directivity of the surface shape. In case $\phi_{S\text{-}C}$ is equal to 0° or 90° (180° or 270°) the method proposed here makes it impossible to give unambiguous information about the directivity of the analysed surfaces, regardless of whether the examined surface is characterised by furrows or not. This imperfection of the method for these $\phi_{S\text{-}C}$ angles can be eliminated if the soil reflectance data are available to be collected in two sets for different horizontal sun angles with their azimuth distance of about 45°.

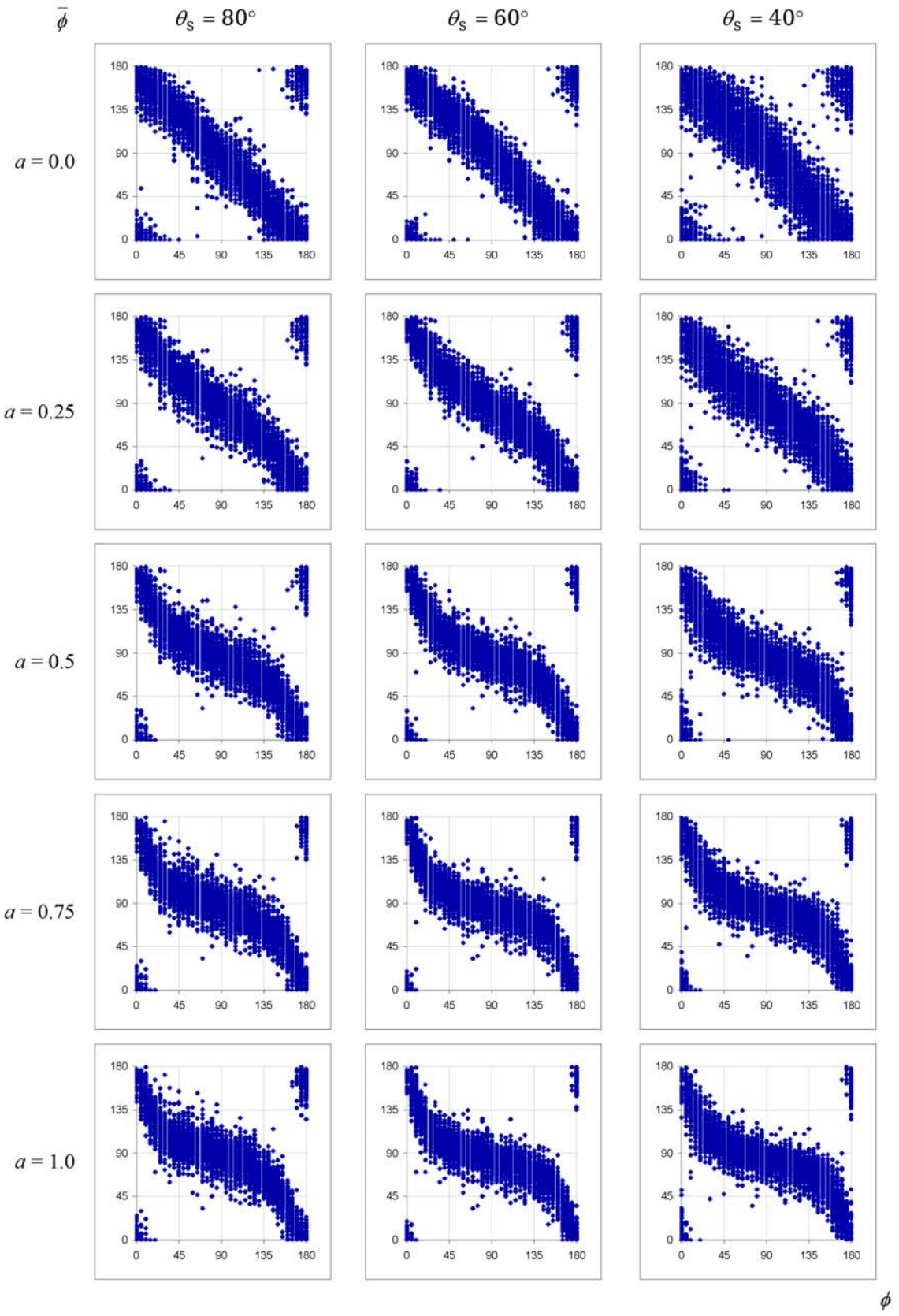

Figure 4. Relation between the angle $\bar{\phi}$ for which the Δ_ϕ reaches its maximal value and the angle $\phi_{S\text{-}C}$ describing the illumination of their furrows as a distance angle between the direction of the furrows and the sun position, established for five soil surfaces with various clarity of their furrows described by the parameter a, illuminated at specified solar zenith angle θ_S.

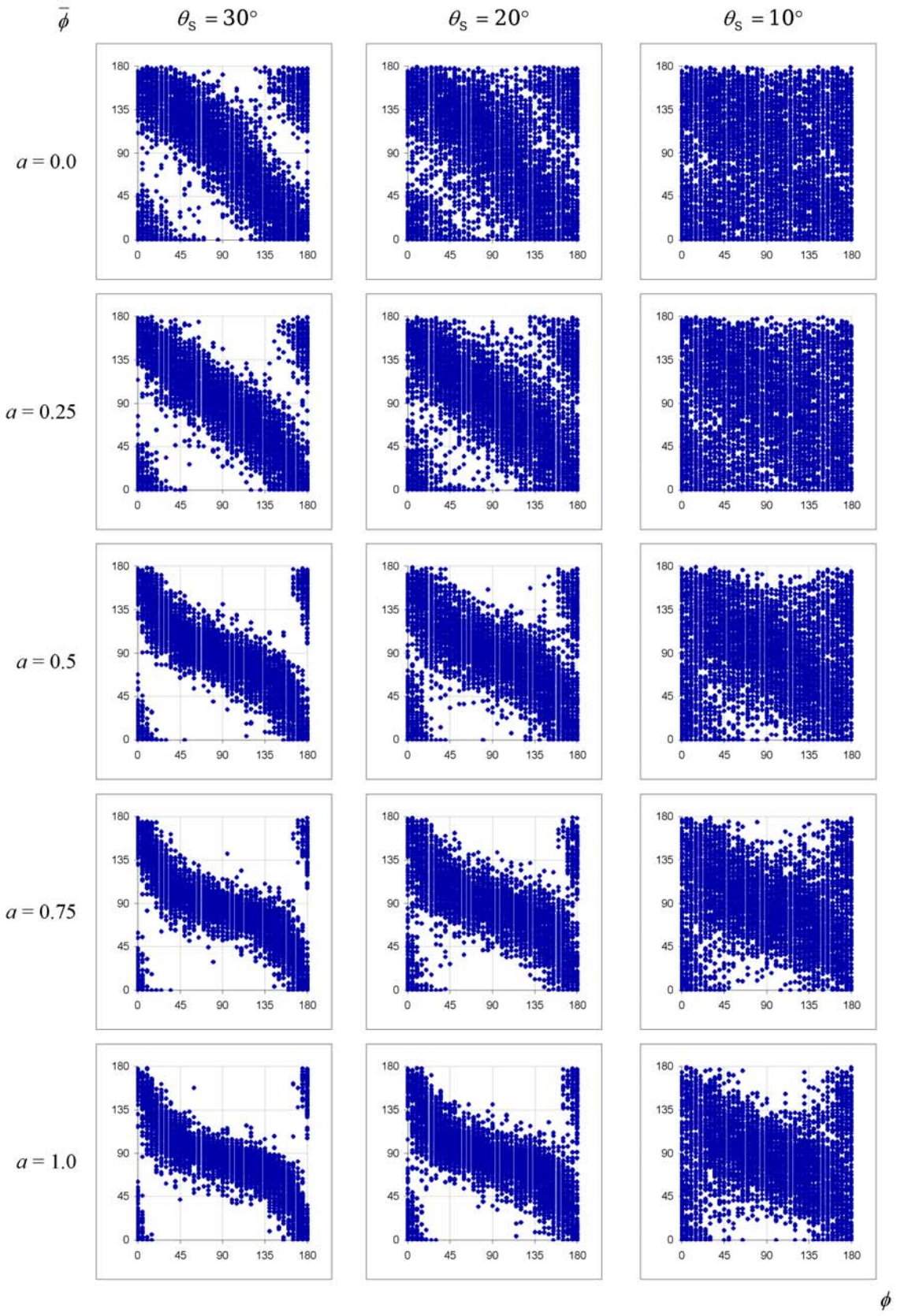

Figure 4. Continued.

CONCLUSIONS

The results of the work confirm our observation reported in our previous paper (i). The method proposed in this paper, using random sampling of the soil hemispherical-directional reflectance, enables us to infer about the directivity of a soil surface at a relatively wide range of the solar zenith angle θ_S, not including the θ_S lower than 30°, even for the surfaces with not so deep furrows.

It is important in practice that these results are satisfied for a relatively small number of the samples.

Undoubtedly, it is necessary to define a quantitative parameter expressing the soil surface directivity with sufficient sensitivity for the method proposed in this paper.

References

i. Cierniewski J, T Gdala & A Karnieli, 2004. A hemispherical-directional reflectance model as a tool for understanding image distinctions between cultivated and uncultivated bare surfaces. Remote Sensing of Environment, 90: 505-523.

ii. Kimes D S, & P J Sellers, 1985. Inferring hemispherical reflectance of the Earth's surface for global energy budget from remotely sensed nadir or directional radiance values. Remote Sensing of Environment, 18: 205-223.

iii. Coulson K L, 1966. Effect of reflection properties of natural surfaces in aerial reconnaissance. Applied Optic. 5: 905-917.

iv. Fraser R S, 1975. Interaction mechanisms – within the atmosphere. In: Manual of Remote Sensing, edited by American Society of Photogrammetry (Falls Church, VA), 181-233.

v. Kondratyev K, 1969. Radiacyonnye kharakteristiki atmosfery i zemnoy poverkhnosti (Gidrometeorologiczeskoye Izdatelstwo, Leningrad) 452 pp.

vi. Abdou W A, J E Conel, S H Pilorz, M C Helmlinger, C J Brugge, B J Gaitley, W C Ledoboer & J V Martonchik, 2001.Vicarious calibration. a reflectance-based experiment with AirMISR. Remote Sensing of Environment, 77: 338-353.

vii. Strub G., M E Schaepman, Y Knyazikhin & K I Itten, 2003. Evaluation of Spectrodirectional alfalfa canopy data acquired during DAISEX'99. IEEE Transaction on Geoscience and Remote Sensing, 41: 1034-1042.

viii. Engelsen O, B Pinty, M M Verstraete & J V Martonchik, 1996. Parametric bidirectional reflectance factor models: evaluation, improvements and applications. Catalogue CL-NA-16426-EN-C (Office for Official Publications of the European Communities, ECSC-EC-EAEC Brussels, Luxembourg), 114 pp.

ix. Grant R H, W Gao & and G M Heisler, 1996. Photosynthetically-active radiation: sky radiance distributions under clear and overcast conditions. Agricultural and Forest Meteorology, 82: 267-292.